This article was downloaded by:
On: *26 January 2011*
Access details: *Access Details: Free Access*
Publisher *Taylor & Francis*
Informa Ltd Registered in England and Wales Registered Number: 1072954 Registered office: Mortimer House, 37-41 Mortimer Street, London W1T 3JH, UK

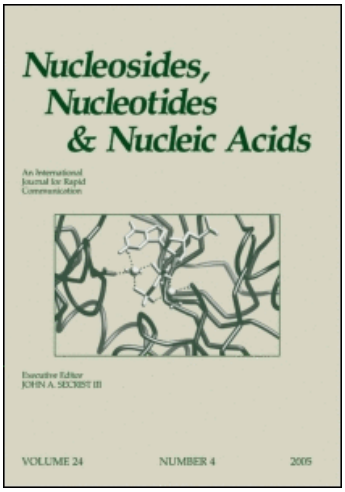

Nucleosides, Nucleotides and Nucleic Acids

Publication details, including instructions for authors and subscription information:
http://www.informaworld.com/smpp/title~content=t713597286

Solution Structure of a GAAG Tetraloop in Helix 6 of SRP RNA from *Pyrococcus furiosus*

Kiyoshi Okada[a]; Mari Takahashi[a]; Taiichi Sakamoto[ab]; Gota Kawai[ab]; Kouji Nakamura[c]; Akio Kanai[d]
[a] Department of Life and Environmental Sciences, Faculty of Engineering, Chiba Institute of Technology, Chiba, Japan [b] Protein Research Group, RIKEN Genomic Sciences Center, Kanagawa, Japan [c] Institute of Biological Sciences, University of Tsukuba, Ibaraki, Japan [d] Institute for Advanced Biosciences, Keio University, Yamagata, Japan

To cite this Article Okada, Kiyoshi , Takahashi, Mari , Sakamoto, Taiichi , Kawai, Gota , Nakamura, Kouji and Kanai, Akio(2006) 'Solution Structure of a GAAG Tetraloop in Helix 6 of SRP RNA from *Pyrococcus furiosus*', Nucleosides, Nucleotides and Nucleic Acids, 25: 4, 383 — 395
To link to this Article: DOI: 10.1080/15257770600683979
URL: http://dx.doi.org/10.1080/15257770600683979

PLEASE SCROLL DOWN FOR ARTICLE

Full terms and conditions of use: http://www.informaworld.com/terms-and-conditions-of-access.pdf

This article may be used for research, teaching and private study purposes. Any substantial or systematic reproduction, re-distribution, re-selling, loan or sub-licensing, systematic supply or distribution in any form to anyone is expressly forbidden.

The publisher does not give any warranty express or implied or make any representation that the contents will be complete or accurate or up to date. The accuracy of any instructions, formulae and drug doses should be independently verified with primary sources. The publisher shall not be liable for any loss, actions, claims, proceedings, demand or costs or damages whatsoever or howsoever caused arising directly or indirectly in connection with or arising out of the use of this material.

Nucleosides, Nucleotides, and Nucleic Acids, 25:383–395, 2006
Copyright © Taylor & Francis Group, LLC
ISSN: 1525-7770 print / 1532-2335 online
DOI: 10.1080/15257770600683979

Taylor & Francis
Taylor & Francis Group

SOLUTION STRUCTURE OF A GAAG TETRALOOP IN HELIX 6 OF SRP RNA FROM *Pyrococcus furiosus*

Kiyoshi Okada and Mari Takahashi □ *Department of Life and Environmental Sciences, Faculty of Engineering, Chiba Institute of Technology, Chiba, Japan*

Taiichi Sakamoto and Gota Kawai □ *Department of Life and Environmental Sciences, Faculty of Engineering, Chiba Institute of Technology, Chiba, Japan, and Protein Research Group, RIKEN Genomic Sciences Center, Kanagawa, Japan*

Kouji Nakamura □ *Institute of Biological Sciences, University of Tsukuba, Ibaraki, Japan*

Akio Kanai □ *Institute for Advanced Biosciences, Keio University, Yamagata, Japan*

Downloaded At: 09:46 26 January 2011

□ *The NMR structure of a 12-mer RNA derived from the helix 6 of SRP RNA from* Pyrococcus furiosus*, whose loop-closing base pair is U:G, was determined, and the structural and thermodynamic properties of the RNA were compared with those of a mutant RNA with the C:G closing base pair. Although the structures of the two RNAs are similar to each other and adopt the GNRR motif, the conformational stabilities are significantly different to each other. It was suggested that weaker stacking interaction of the GAAG loop with the U:G closing base pair in 12-mer RNA causes the lower conformational stability.*

Keywords SRP; GNRR motif

INTRODUCTION

The signal recognition particle (SRP) is a ubiquitous ribonucleoprotein particle found in all three domains of life, which plays an important role in the co-translational translocation of secretory proteins across the membrane.[1] Mammalian SRP consists of SRP RNA and six proteins (SRP9/14, SRP19,

Received 14 December 2005; accepted 19 January 2006.
This work was supported by Grants-in-Aid for Scientific Research on Priority Areas (14035205) and, in part, by High Technology Research and from the Ministry of Education, Culture, Sports, Science and Technology (MEXT) of Japan, and by the RIKEN Structural Genomics/Proteomics Initiative (RSGI), the National Project on Protein Structural and Functional Analyses of MEXT.
This article is dedicated to Professor Eiko Ohtsuka on the occasion of her 70th birthday.
Address correspondence to Gota Kawai, Department of Life and Environmental Sciences, Faculty of Engineering, Chiba Institute of Technology, 2-17-1 Tsudanuma, Narashino-shi, Chiba 275-0016, Japan. E-mail: gkawai@sea.it-chiba.ac.jp

SRP54, and SRP68/72), and the mammalian SRP RNA consists of six helical domains (helix 2-8). The RNA component (helix 1-6 and 8, Figure 1A) of archaeal SRP is almost similar in size and secondary structure to its mammalian counterpart, while only two protein homologues, SRP54 and SRP19, have been identified so far in archaeal genomes.[2,3] In the assembly of SRP particle, prior binding of SRP19 to the helices 6 and 8 of SRP RNA is required for further binding of SRP54, which binds to the signal sequence, to the helix 8 in the case of human and *Archaeoglobus fulgidus* (Archaea).[4] In contrast, SRP54 from *Pyrococcus furiosus* and *Methanococcus jannaschii* (Archaea) can bind to SRP RNA in the absence of SRP19.[5,6] Structures of SRP and its components are extensively characterized by the X-ray crystallography and NMR spectroscopy.[7–23] SRP19 interacts with the major groove of the helix 6 tetraloop and the minor groove of the helix 8 tetraloop and these interactions induces the interaction between the tetraloops of helices 6 and 8 in human SRP.[21] Similar interactions were also found in *M. jannaschii*

Downloaded At: 09:46 26 January 2011

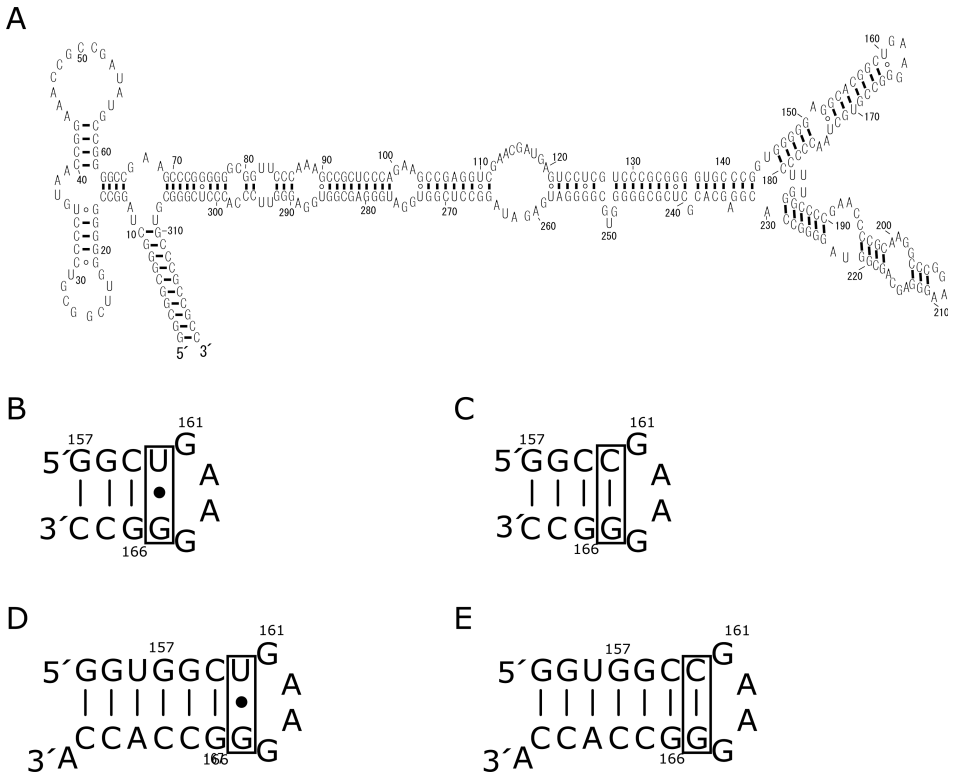

FIGURE 1 Secondary structures of RNAs. (A) Secondary structure of *Pyrococcus furiosus* SRP RNA. (B) Secondary structure of pfHE6-12 (12 mer) used for the structure determination. (C) Secondary structure of a mutant of pfHE6-12, pfHE6-12M, used for the comparison with pfHE6-12. Longer RNAs, pfHE6-19 (D) and pfHE6-19M (E), were designed for the efficient incorporation of ^{13}C- and ^{15}N-labeled guanosine residues.

SRP RNA.[22,23] Thus, the helix 6 plays an important role in the assembly of SRP.

The GNAR sequences are found in 95% of the loop sequences in helix 6 from Eukarya and Archaea.[2,7,24] However, the loop-closing base pairs of the helix 6 show the interesting tendency; the population of the closing base pairs of GNAR loops in the helix 6 are C:G (30%), U:A (17%), A:U (27%), G:C (21%), and U:G (5%) for Eukarya and C:G (41%), U:A (14%), and U:G (45%) for Archaea (SRPDB: the version of September 27, 2005).[2] We have determined the solution structure of the helix 6 of human SRP RNA and found that the GGAG loop in the helix 6 of human SRP RNA adopts the GNRR structural motif which is an extended GNRA motif.[7] The closing base pair of human helix 6 is G:C. In this study, we determined the NMR structure of a 12-mer RNA (pfHE6-12) comprising the hairpin loop of the helix 6 from *P. furiosus* (Figure 1B), having a GAAG loop and a U:G closing base pair, in order to analyze the effect of the closing base pairs on the loop structure. This is the first solution structure of a GNRR loop with a U:G closing base pair. We also compared NMR spectra and thermal melting profile of pfHE6-12 with those of a mutant having a C:G closing base pair (pfHE6-12M, Figure 1C). The influence of closing base pair on stability, RNA-RNA interaction and conformation of the GNRR loop is discussed.

Downloaded At: 09:46 26 January 2011

MATERIALS AND METHODS

RNA Synthesis, Purification, and Preparation

The RNA fragments, pfHE6-12, and pfHE6-12M were chemically synthesized by the phosphoramidite method, using an automatic DNA/RNA synthesizer, Expedite model 8909 (PerSeptive Biosystems, MA). Furthermore, to confirm the NMR signal assignments of guanosine residues in the loop regions, ^{13}C- and ^{15}N-labeled guanosine residues ([G-^{13}C/^{15}N]) were incorporated into 19-mer RNA samples, which have 3 additional base pairs and an additional adenosine residue at the 3′ terminal (pfHE6-19 and pfHE6-19M, Figures 1D and 1E) to increase the efficiency of *in vitro* transcription reaction. For stable-isotopic labeling, ^{13}C- and ^{15}N-labeled GTP (Taiyo Nippon Sanso, Tokyo, Japan) were used. Purification of RNA samples were performed with the polyacrylamide gel electrophoresis (PAGE) under the denaturing conditions. Conformations of RNA samples were monitored by the 20% non-denaturing PAGE. For the NMR measurements, RNA samples were dissolved in 20 mM sodium phosphate buffer (pH 6.5) containing 50 mM NaCl. The final concentrations of pfHE6-12 and pfHE6-12M were 2.0 mM and 1.0 mM, respectively. The concentrations of [G-^{13}C/^{15}N] pfHE6-19M as well as [G-^{13}C/^{15}N] pfHE6-19 were 0.5 mM. To confirm the monomer hairpin structure, the samples were subjected to the non-denaturing PAGE analysis before and after the NMR and UV-melting experiments.

Measurements and Analyses of NMR Spectra

NMR spectra were measured on DRX-500 and DRX-600 spectrometers (BRUKER Biospin). Spectra were recorded at 7–30°C and the NMR data at 10°C were used for the structure calculation. The exchangeable proton resonances were obtained with the 2D-NOESY (2048 × 512 complex points, 256 scans), and ^{1}H-^{15}N HSQC experiments (2048 × 512 complex points, 200 scans) using the jump-and-return scheme with gradient pulses for water suppression. The non-exchangeable proton resonances were obtained with the 2D-NOESY (2048 × 2048 complex points, 64 scans), 2D-TOCSY (2048 × 1024 complex points, 8 scans), 2D-DQF-COSY (2048 × 2048 complex points, 32 scans), natural-abundance ^{13}C-^{1}H HSQC (2048 × 256 complex points, 512 scans), and ^{13}C-^{1}H HSQC experiments (2048 × 256 complex points, 8 scans). The 2D-NOESY (H_2O and D_2O), 2D-TOCSY, and 2D-DQF-COSY natural-abundance ^{13}C-^{1}H HSQC spectra were measured using the 12-mer RNA samples. The ^{15}N-^{1}H HSQC and ^{13}C-^{1}H HSQC spectra were measured using the [G-^{13}C/^{15}N] 19-mer RNA samples.

Downloaded At: 09:46 26 January 2011

Exchangeable proton resonances were assigned by the NOESY spectrum with a mixing time of 150 ms in H_2O. Well-established procedures were used for resonance assignments for non-exchangeable protons.[25] Assignments of H2 protons of adenosine and H1′ protons of guanosine were confirmed by the ^{13}C-^{1}H HSQC spectrum obtained using natural-abundance ^{13}C.[26] NOE distance restraints for non-exchangeable protons were obtained using the NOESY spectra (mixing times of 100 and 400 ms) in D_2O.[27] NOE intensities from exchangeable protons were interpreted as distances of 0–3.5 Å (strong) or 0–6 Å (weak), while NOE intensities from non-exchangeable protons were interpreted as distances of 0–3 Å (strong), 0–4 Å (medium), 0–5 Å (weak), or 0–7 Å (very weak). In order to estimate the dihedral angle, sugar pucker was analyzed using the TOCSY and DQF-COSY spectra. A small $^{3}J_{H1'-H2'}$ and a large $^{3}J_{H3'-H4'}$ values correspond to the C3′-*endo* conformation ($\delta = 85^{\circ} \pm 30^{\circ}$).[28]

Structure Calculation of pfHE6-12

A set of 100 structures was calculated using a simulated annealing protocol with the InsightII/Discover package. The amber force filed was used. A total of 127 NOE distance restraints including the five restraints for the absence of NOE cross peaks, 34 dihedral restraints, and 18 hydrogen bonding restraints were used. The force constants were 100 kcal mol^{-1} Å^{-2} for distance restraints and 100 kcal mol^{-1} rad^{-2} for dihedral restraints. The starting coordinates were randomized and then heated to 2000 K over 5 ps, and the temperature maintained at 2000 K for another 5 ps. After all restraints were increased to full value over 20 ps, they were decreased to 10% of full

value over 5 ps. The van der Waals radius was increased from 10 to 82.5% over 20 ps. All restraints were increased to full value over 10 ps again. The nonbond scale was increased to full value over 20 ps. The temperature was kept at 2000 K for another 5 ps. The temperature was then scaled to 300 K over 10 ps. After the structure was heated from 300 to 1000 K over 5 ps, the van der Waals radius was increased from 82.5% to full value over 5 ps, after which it was decreased from full to 82.5% over 5 ps. An additional 5 ps of dynamics was performed at 1000 K, and the temperature was scaled to 300 K over 10 ps. Total simulation time was 130 ps. A final minimization was performed, which included a Lennard-Jones potential and electrostatic terms with a dielectric constant of 7. The 12 final structures having the lowest total energy were chosen.

The Melting Profiles of pfHE6-12 and pfHE6-12M

UV absorbance melting profiles at 260 nm were obtained using a DU-640 (Beckman Coulter). RNA samples were dissolved in 325 μl of 20 mM sodium phosphate buffer (pH 6.5) containing 50 mM NaCl. Two samples with different RNA concentrations were prepared for each RNA to check the concentration dependences. The concentrations of pfHE6-12 were 0.9 μM and 4.0 μM, and the concentrations of pfHE6-12M were 1.0 μM and 1.6 μM. The temperature was raised from 25 to 100°C at a heating rate of 1°C min^{-1}. Melting temperature (T_m value) was obtained by the derivative plot with an averaging of 5 points.

Downloaded At: 09:46 26 January 2011

RESULTS

Analysis of Exchangeable Proton Resonances

The imino proton resonances of pfHE6-12 and pfHE6-12M were assigned on the basis of the NOESY spectra observed in H_2O. For pfHE6-12, the imino proton resonances of the U:G base pair, U160:G165, were identified by their unique chemical shifts (10.6 and 11.7 ppm) and a strong intra-base pair NOE. Starting from these unique resonances, resonances are sequentially assigned by NOE connectivities as U160/G165-G166, G158-G157. The imino proton resonances of G157 (12.4 ppm) and G158 (13.4 ppm) in pfHE6-12M were observed at the nearly same chemical shifts as is the case of pfHE6-12. Furthermore, a similar NOE connectivity, G165-G166-G158, was observed for pfHE6-12M. Thus, assignment of the imino proton resonances proves the formation of the predicted base pairs in these constructs. With the imino proton resonances assigned, cytosine amino proton resonances were unambiguously assigned on the basis of their strong NOEs to the imino protons of the base-paired guanosine residue.

On the basis of similarities to the previous study of GGAG loop in human helix 6,[7] we assigned the resonances at 10.0 and 6.1 ppm for pfHE6-12 and at 9.7 and 6.0 ppm for pfHE6-12M to the imino and N2 amino protons of G161, respectively, which was supported by ^{15}N-^{1}H HSQC spectra of [G-^{13}C/^{15}N] pfHE6-19 and [G-^{13}C/^{15}N] pfHE6-19M. It is notable that one N2 amino proton signal of G161 could be observed for both pfHE6-12 and pfHE6-12M, although signals of guanosine N2 amino protons are generally not observed due to the fast exchange process. Furthermore, NOEs between the imino and amino protons of G161 support the validity of the assignments. A strong NOE between the amino proton of G161 and the H8 proton of G164 for pfHE6-12 (Figure 2A) as well as pfHE6-12M (Figure 2B) suggested the formation of G:G base pairs similar to that found in the GGAG loop of human helix 6.[7]

Analysis of Non-Exchangeable Proton Resonances

The non-exchangeable proton resonances of pfHE6-12 and pfHE6-12M observed in D_2O were assigned by the conventional method.[25] Figures 2C and 2D show the sequential assignment of the NOE crosspeaks (H8/H6-H1′) for pfHE6-12 and pfHE6-12M, respectively. The natural-abundance ^{13}C-^{1}H HSQC experiments for 12-mer RNAs and ^{13}C-^{1}H HSQC experiments for [G-^{13}C/^{15}N] 19-mer RNAs assist the assignment of the H2′ and H3′ proton resonances. In the TOCSY and DQF-COSY spectra, no signals derived from large $^{3}J_{\mathrm{H1'-H2'}}$ were observed, indicating that all nucleotides in pfHE6-12 and pfHE6-12M adopt the C3′-*endo* conformation.[28]

The signals with unusual upfield chemical shifts, 4.34 and 4.48 ppm for pfHE6-19 and pfHE6-19M, respectively, were confirmed to be due to H1′ of G165 by the ^{13}C-^{1}H HSQC spectra based on the ^{13}C chemical shifts (Figures 2E and 2F). It was also reported that the chemical shifts of H1′ at the corresponding residue in GNRR loops were 3.5–4.5 ppm,[7,8,29] and these protons are suggested to experience the strong ring current effects of the fourth base in GNRR loops. Since unusual chemical shifts are sensitive indicators for unusual local structure, observation of similar unusual chemical shifts in each H1′ of GNRR loops suggested that these tetraloops are structurally similar to each other.

Structure Determination of pfHE6-12

The structure of pfHE6-12 was determined using the conventional method.[7,25] A total of 127 NOE and 34 dihedral angle restraints were obtained from NMR data. The structures were calculated using the restrained molecular dynamics in a simulated annealing protocol. A total of 12 structures converged to low total energy (Figure 3). The structures were well defined by NMR data with a heavy atom root-mean-square deviation (r.m.s.d.)

Downloaded At: 09:46 26 January 2011

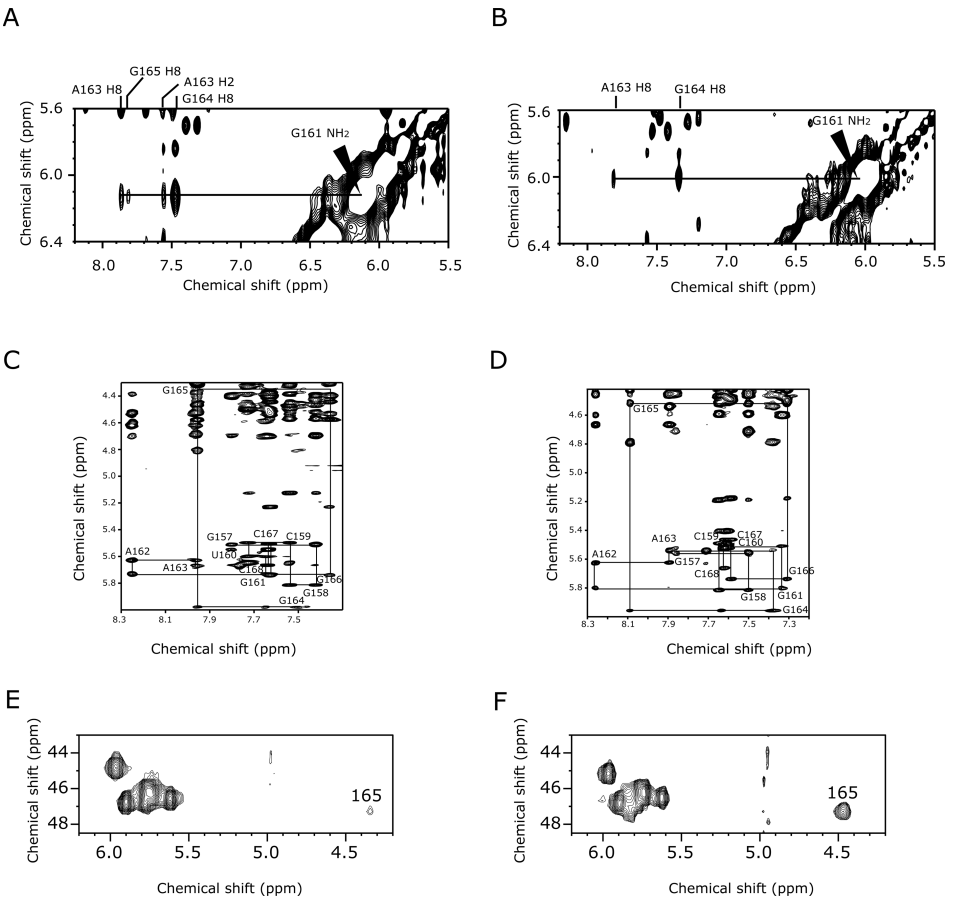

FIGURE 2 NMR spectra of RNAs. 2D NOESY spectra of pfHE6-12 (A) and pfHE6-12M (B) measured in H_2O (a mixing time of 150 ms) at 15°C. Chemical shift of G161 amino proton is indicated by a horizontal line. Related NOE cross-peaks are labeled with the name of the connected proton. 2D NOESY spectra of pfHE6-12 (C) and pfHE6-12M (D) in D_2O (a mixing time of 400 ms) at 10°C, showing cross-peaks between aromatic H6 or H8 protons and ribose H1′ protons. Sequential connectivities are indicated by lines and intra-residue NOEs are labeled by residue names. 2D HSQC spectra of pfHE6-19 (E) and pfHE6-19M (F) in D_2O at 10°C. The signals for H1′ of G165 were indicated.

for the 12 structures of 1.02 Å (Table 1). The converged structures did not contain experimental distance violation of >0.2 Å or dihedral violation of >3°.

The structure of the GAAG loop (U160-G165), which contains noncanonical G:G base pair, was well converged (heavy atoms r.m.s.d. was 0.90 Å). The G161:G164 base pair (Figure 4B) can be categorized as a single bond mismatch: sugar-edge/Hoogsteen-edge [nomenclature proposed by N.B. Leontis and E. Westhof[30]]. The N2 amino group of G161 forms a hydrogen bond with the N7 of G164 (2.23 Å), which is consistent with an NOE crosspeak

Downloaded At: 09:46 26 January 2011

TABLE 1 NMR Restraints and Structural Statistics

Number of experimental restraints	
Distance restraints	127
Dihedral restraints	34
Hydrogen bonding distance restraints	18
R.m.s. deviation from restraints	
Distance restraints (Å)	0.0111 ± 0.0016
Dihedral restraints (°)	0.23 ± 0.09
R.m.s. deviation from idealized geometry	
Bonds (Å)	0.0082 ± 0.0005
Angle (°)	2.38 ± 0.19
Impropers (°)	1.6 ± 0.4
Heavy-atoms r.m.s. deviation (Å)[a]	
All	1.02
Loop (U160-G165)	0.90
Stem (G157-C159, G166-C168)	0.89

[a]Averaged r.m.s.d. between an average structure and the 12 converged structures were calculated. The converged structures did not contain experimental distance violation of >0.2 Å or dihedral violation of >3°.

Downloaded At: 09:46 26 January 2011

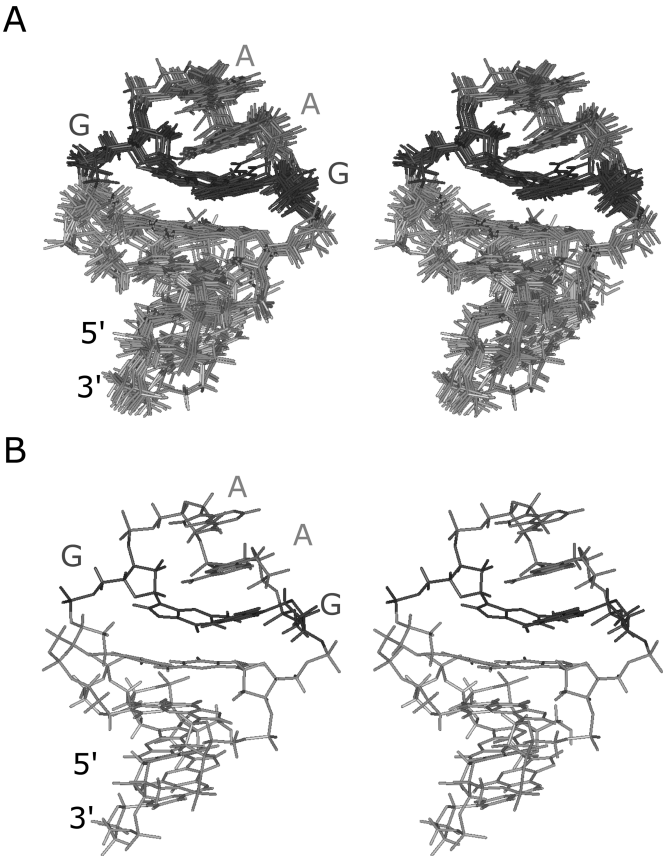

FIGURE 3 Solution structures of pfHE6-12 determined by NMR. (A) Stereo view of the superposition of final 12 structures of pfHE6-12. (B) Stereo view of the minimized average structure of pfHE6-12.

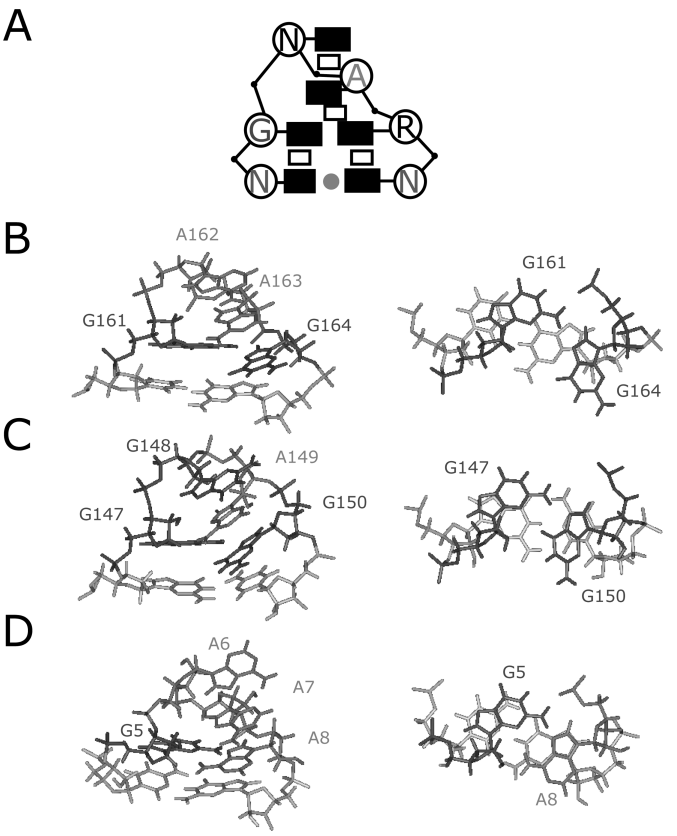

FIGURE 4 The GNRR loops and G:R mismatches. Original residue number was used for each structure. (A) The schematic representation of the GNRR tetraloop. The following symbols are used in the schematic representation: black rectangle, base; open rectangle, stacking interaction; grey circle, hydrogen bonding interaction; open circle, ribose. (B) The GAAG loop structure in *P. furiosus* helix 6 (in the present structure) and the G:G mismatch. (C) The GGAG loop structure in human SRP RNA (PDB ID: 1L1W) and the G:G mismatch. (D) The GAAA loop structure in *E. coli* 16S rRNA (PDB ID: 1ZIF) and the G:A mismatch.

between the N2 amino proton of G161 and H8 proton of G164. G161 is stacked on U160:G165 base pair and a sharp turn in the phosphodiester backbone occurs between G161 and A162. The three nucleotides A162-G164 are continuously stacked as schematically shown in Figure 3B. The structure qualitatively explains the unusual chemical shift of H1′ of G165, which is shifted upfield slightly by the ring current of the guanosine base of G164.

The Melting Profiles of pfHE6-12 and pfHE6-12M

The melting profiles indicating the hairpin-to-random chain transition are shown in Figure 5. Either of pfHE6-12 or pfHE6-12M shows no concentration dependence in the range of 0.9 to 4.0 μM (data not shown). By the derivative plot, the T_m values of pfHE6-12 and pfHE6-12M were determined

Downloaded At: 09:46 26 January 2011

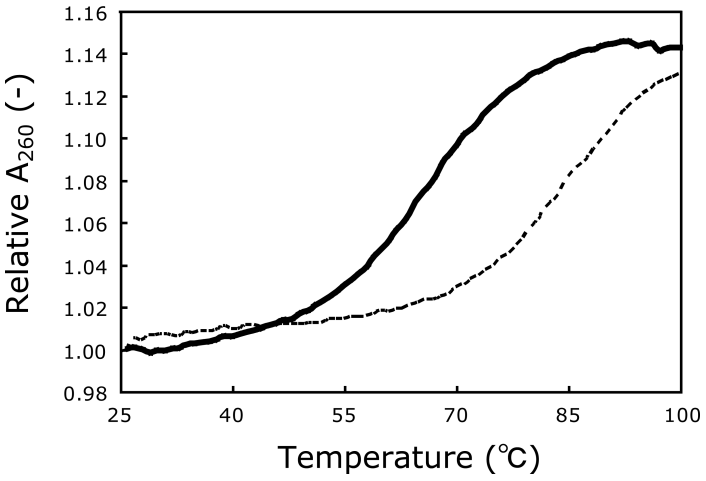

FIGURE 5 The melting profiles of RNAs. The pfHE6-12 and pfHE6-12M are indicated by solid and dot lines, respectively. UV absorption was normalized by the values at 25°C.

Downloaded At: 09:46 26 January 2011

to be 66 and 86°C, respectively. Thus, it was found that T_m value of pfHE6-12M was significantly higher than that of pfHE6-12. Interestingly, the hyperchromicity values were estimated to be 12% for both pfHE6-12 and pfHE6-12M. In combination with the fact that the structures of pfHE6-12 and pfHE6-12M are similar to each other as described above, the same process of the structural change is shared for these two hairpins while the stabilities are significantly different to each other.

DISCUSSION

It was shown that the structural characteristics of the pfHE6-12 and pfHE6-12M are similar to each other. Furthermore, the structural characteristics of the pfHE6-12 and pfHE6-12M are similar to those of other tetraloops of the GNRR motif such as the GGAG loop of helix 6 of human SRP RNA (PDB ID: 1L1W; r.m.s.d. for the 15 structures of 1.18 Å, Figure 4C) or the GAAA loop of 16S rRNA (PDB ID: 1ZIF; r.m.s.d. for the 10 structures of 0.67 Å, Figure 4D).[7,31] It has been found that the CACG tetraloop with wobble U:G closing base pair from coxsackievirus B3 (PDB ID: 1RFR) adopts YNMG tetraloop motif (M is either a C or an A) such as cUUCGg tetraloop.[32] Thus, it was suggested that the wobble U:G closing base pair is a possible alternative to the Watson-Crick closing base pair for maintaining the structural features of the stable tetraloops such as GNRR and YNMG motif.

Although the general structural features are shared among the GNRR tetraloops, the location of the fourth G in the GAAG loop of pfHE6-12 is slightly different from those of other GNRR loops (Figures 4B, C, and D). In the GAAG loop of pfHE6-12, G161 is stacked on U160:G165 base pair, which

is consistent with an NOE crosspeak between an amino proton of G161 and H8 proton of G165 (Figure 2A), and G164 slide out toward the minor groove. In contrast, in the case of the GGAG loop of helix 6 of human SRP RNA with the G:C closing base pair (Figure 4C), the fourth G (G150) stacked to the adjacent C151 and, in the case of the GAAA loop of *E. coli* 16S rRNA with the C:G closing base pair (Figure 4D), the fourth A (A8) is partially stacked to the adjacent G9. Thus, it was suggested that stacking interaction of the fourth G in the GAAG loop of pfHE6-12 is slightly weak compare to those of the other GNRR loop. Because pfHE6-12M, whose closing base pair is C:G, may share the similar stacking interaction with the GAAA loop of *E. coli* 16S rRNA, the difference in the stacking interactions may be one of the reason for the significant lower T_m value for pfHE6-12. The lower stability of the U:G base pair than the C:G base pair may also the reason. However, it has also reported that the loop closed by G:U is more stable than the loops closed by G:C or C:G.[33–35] Thus, the difference of the conformational stability between pfHE6-12 and pfHE6-12M are mainly caused by the weak stacking interaction around G165 in pfHE6-12.

Some binding experiments suggested that SRP54 can bind to the helix 8 without SRP19 in the case of *M. jannaschii* and *P. furiosus*, whereas SRP54 binding to the helix 8 of SRP RNA requires prior binding of SRP19 to the helix 6 in the case of human and *A. fulgidus*.[4] The closing base pairs of the tetraloop of the helix 6 from both of *M. jannaschii* and *P. furiosus* are U:G, while those from human and *A. fulgidus* are G:C and C:G, respectively. Recent structural studies of SRP RNA-SRP19 complexes from human and *M. jannaschii* have revealed that SRP19 binds to the helix 6 through contact with the phosphodiester backbone of the tetraloop, which induces a loop-loop interaction between the helices 6 and 8 in SRP RNA.[22,23] Furthermore, the crystal structure of S-domain in SRP RNA from *M. jannaschii* revealed that the loop-loop interaction between the helices 6 and 8 occurs without SRP19. Thus, the loop-loop interaction, which is accomplished by the two minor-groove base triples including third and forth base in the tetraloop of the helix 6, was suggested to induce conformational change suitable for SRP54 binding to the helix 8. Nevertheless, the fourth base of GGAG loop in human helix 6 showed large stacking in the free RNA,[7] the fourth base (G164) of GAAG loop in *P. furiosus* helix 6 was suggested to be pushed out toward the minor groove (Figure 4B). Thus, the U:G closing base pair of tetraloops in helix 6 might induce an open conformation of the loop, which was thought to give rise to the loop-loop interaction important for SRP54 binding.

Downloaded At: 09:46 26 January 2011

Database Deposition

The chemical shift assignments have been deposited in the Biological Magnetic Resonance Data Bank (accession code 10014) and the structure has been deposited in the Protein Data Bank (accession code 2F87).

REFERENCES

1. Lütcke, H. Signal Recognition Particle (SRP), a Ubiquitous Initiator of Protein Translocation. European Journal of Biochemistry **1995**, 228, 531–550.
2. Rosenblad, A.M.; Gorodkin, J.; Knudesen, B.; Zwieb, C.; Samuelsson, T. SRPDB: Signal recognition particle database. Nucleic Acids Research **2003**, 31, 363–364.
3. Zwieb, C.; Nues, R.W.V.; Rosenblad, A.M.; Brown, D.J.; Samuelsson, T. A nomenclature for all signal recognition particle RNAs. RNA **2005**, 11, 7–13.
4. Bhuiyan, H.S.; Gowda, K.; Hotokezaka, H.; Zwieb, C. Assembly of archaeal signal recognition particle from recombinant components. Nucleic Acids Research **2000**, 28, 1365–1373.
5. Maeshima, H.; Okuno, E.; Aimi, T.; Morinaga, T.; Itoh, T. An archaeal protein homologous to mammalian SRP54 and bacterial Ffh recognizes a highly conserved region of SRP RNA. FEBS Letters **2001**, 507, 336–340.
6. Yin, J.; Yang, C.H.; Zwieb, C. Assembly of human signal recognition particle (SRP): Overlap of regions required for binding of protein SRP54 and assembly control. RNA **2001**, 7, 1389–1396.
7. Sakamoto, T.; Morita, S.; Tabata, K.; Nakamura, K.; Kawai, G. Solution structure of a SRP19 binding domain in human SRP RNA. Journal of Biochemistry **2002**, 132, 177–182.
8. Schmitz, U.; James, T.L.; Lukavsky, P.; Walter, P. Structure of the most conserved internal loop in SRP RNA. Nature Structural Biology **1999**, 6, 634–638.
9. Rosendal, K.R.; Wild, K.; Montoya, G.; Sinning, I. Crystal structure of the complete core of archaeal signal recognition particle and implication for interdomain communication, Proceedings of the National Academy of Sciences of the United States of America. **2003**, 100, 14701–14706.
10. Birse, D.E.; Kapp, U.; Strub, K.; Cusack, S.; A-ring, A. The crystal structure of the signal recognition particle *Alu* RNA binding heterodimer, SRP9/14. EMBO Journal **1997**, 16, 3757–3766.
11. Weichenrieder, O.; Wild, K.; Strub, K.; Cusack, S. Structure and assenmbly of the *Alu* domain of the mammalian siganl recognition particle. Nature **2000**, 408, 167–73.
12. Keenan, R.J.; Freymann, D.M.; Walter, P.; Stroud, R.M. Crystal structure of the signal sequence binding subunit of the signal recognition particle. Cell **1998**, 94, 181–191.
13. Clemons, W.M. Jr.; Gowda, K.; Black, S.D.; Zwieb, C.; Ramakrishnan, V. Crystal structure of the conserved subdomain of human protein SRP54M at 2.1 Å Resolution: evidence for the mechanism of signal peptide binding. Journal of Molecular Biology **1999**, 292, 697–705.
14. Schmitz, U.; Behrens, S.; Freymann, D.M.; Keenan, R.J.; Lukavsky, P.; Walter, P.; James, T.L. Structure of the phylogenetically most conserved domain of SRP RNA. RNA **1999**, 5, 1419–1429.
15. Jovine, L.; Hainz, T.; Oubridge, C.; Scott, W.G.; Li, J.; Sixma, T.K.; Wonacott, A.; Skarzynski, T.; Nagai, K. Crystal structure of the Ffh and EF-G binding sites in the conserved domain IV of *Escherichia coli* 4.5S RNA. Structure **2000**, 8, 527–540.
16. Wild, K.; Weichenrieder, O.; Leonard, G.A.; and Cusack, S. The 2 Å structure of helix 6 of the human signal recognition particle RNA. Struct. Fold. Des. **1999**, 7, 1345–1352.
17. Batey, R.T.; Rambo, R.P.; Lucast, L.; Rha, B.; Doudna, J.A. Crystal structure of the ribonucleoprotein core of the signal recognition particle. Science **2000**, 287, 1232–1239.
18. Pakhomova, O.N.; Deep, S.; Huang, Q.; Zwieb, C.; Hinck, A.P. Solution structure of protein SRP19 of *Archaeoglobus fulgidus* signal recognition particle. Journal of Molecular Biology **2002**, 317, 145–158.
19. Wild, K.; Sinning, I.; Cusack, S. Crystal structure of an early protein-RNA assembly complex of the signal recognition particle. Science **2001**, 294, 598–601.
20. Oubridge, C.; Kuglstatter, A.; Jovine, L.; Nagai, K. Crystal structure of SRP19 in complex with the S domain of SRP RNA and its implication for the assembly of the signal recognition particle. Molecular Cell **2002**, 9, 1251–1261.
21. Kuglstatter, A.; Oubridge, C.; Nagai, K. Induced structural changes of 7Sl RNA during the assembly of human signal recognition particle. Nature Structural Biology **2002**, 9, 740–744.
22. Hainzl, T.; Huang, S.; Sauer-Eriksson, A.E. Structure of the SRP19-RNA complex and implications for signal recognition particle assembly. Nature **2002**, 417, 767–771.
23. Hainzl, T.; Huang, S.A.; Sauer-Eriksson, E. Structural Insights into SRP RNA: An induced fit mechanism for SRP assembly. RNA **2005**, 11, 1043–1050.
24. Zwieb, C. Conformity of RNAs that interact with tetranucleotide loop binding proteins. Nucleic Acids Research **1992**, 20, 4397–4400.
25. Allain, F.H.; Varani, G. Structure of the P1 Helix from group I self-splicing introns. Journal of Molecular Biology **1995**, 250, 333–353.

Downloaded At: 09:46 26 January 2011

26. Legault, P.; Farmer II, B.T.; Mueller, L.; Pardi, A. Throughbond correlation of adenine protons in a ^{13}C-labeled ribozyme. Journal of the American Chemical Society **1994**, 116, 2203–2204.
27. Jeener, J.; Meier, B.H.; Bachmann, P.; Ernst, R.R. Investigation of exchange processes by two-dimensional NMR spectroscopy. Journal of Physical Chemistry **1979**, 71, 4546–4553.
28. Altona, C.; Sundaralingam, M. Conformational analysis of the sugar ring in nucleosides and nucleotides. Improved Method for the Interpretation of Proton Magnetic Resonance Coupling Constants. Journal of the American Chemical Society **1973**, 95, 2333–2344.
29. Legault, P.; Hoogstraten, C.G.; Metlitzky, E.; Pardi, A. order, dynamics and metal-binding in the lead-dependent ribozyme. Journal of Molecular Biology **1998**, 284, 325–335.
30. Leontis, N.B.; Westhof, E. Geometric nomenclature and classification of RNA base pairs. RNA **2001**, 7, 499–512.
31. Jucker, F.M.; Heus, H.A.; Yip, P.F.; Moors, E.H.; Pardi, A. A network of heterogeneous hydrogen bonds in GNRA tetraloops. Journal of Molecular Biology **1996**, 264, 968–980.
32. Du, Z.; Yu, J.; Andino, R.; James, T.L. Extending the Family of UNCG-like Tetraloop Motifs: NMR structure of a CACG tetraloop from coxsackievirus B3. Biochemistry **2003**, 42, 4373–4383.
33. Martin, J.S.; Matthew, H.L.; Theresa, J.A.; Calvin, A.S.; Douglas, H.T. RNA hairpin loop stability depends on closing base pair. Nucleic Acids Research **1993**, 21, 3845–3849.
34. SantaLucia, Jr., J.; Kierzek, R.; Turner, D.H. Functional group substitutions as probes of hydrogen bonding between GA mismatches in RNA internal loops. Journal of the American Chemical Society **1991**, 113, 4313–4322.
35. Turner, D.H.; Sugimoto, N.; Kierzek, R.; Dreiker, S.D. Free energy increments for hydrogen bonds in nucleic acid base pairs. Journal of the American Chemical Society **1987**, 109, 3783–3785.

Downloaded At: 09:46 26 January 2011